

Invisible flat bands on a topological chiral edge

Youjiang Xu, Irakli Titvinidze, Walter Hofstetter

Goethe-Universität Frankfurt, Institut für Theoretische Physik, 60438 Frankfurt am Main, Germany

We prove that invisible bands associated with zeros of the single-particle Green's function exist ubiquitously at topological interfaces of 2D Chern insulators, dual to the chiral edge/domain-wall modes. We verify this statement in a repulsive Hubbard model with a topological flat band, using real-space dynamical mean-field theory to study the domain walls of its ferromagnetic ground state. Moreover, our numerical results show that the chiral modes are split into branches due to the interaction, and that the branches are connected by invisible flat bands. Our work provides deeper insight into interacting topological systems.

Flat bands are sensitive to interaction due to their vanishing band width. For example, it is one of a few rigorous theorems regarding the Hubbard model that, along with flat bands, even the weakest interaction can induce a ferromagnetic ground state [1–6]. Things become even more interesting when the underlying flat bands have non-trivial topology. Researchers have extensively studied two-dimensional (2D) systems in which the interplay between flat Chern bands and interaction leads to quantum Hall ferromagnets [7–9], non-abelian fractional Chern insulators [10–14], novel spin excitations [15, 16] and topologically protected chiral valley channels [17]. Nevertheless, new physics can emerge from this well-studied platform.

In this Letter, we report the emergence of invisible flat bands in the domain-wall spectrum of a 2D quantum Hall ferromagnet resulting from the interplay of the Hubbard interaction and the topological flat band. In a many-body fermionic system, an invisible state associated with a certain characteristic frequency is a special single-particle state being a null vector of the single-particle Green's function of the system at that frequency. An invisible flat band is a collection of invisible states with different momenta and the same characteristic frequency. The existence of invisible states was first studied by Gurarie [18], who pointed out that a closed and non-interacting system doesn't possess an invisible state, and predicted that the existence of invisible states may alter the edge-bulk correspondence of topological insulators in the way that the topological invariant could possibly change without closing the gap [18]. Despite the interesting properties of invisible states, they are not well studied. In this Letter, we will present two important results about them. One is a proof that invisible bands exist ubiquitously at topological interfaces of 2D Chern insulators, which implies that they can serve as topological markers in such systems, and the other is the aforementioned emergence of invisible flat bands.

We study the quantum Hall ferromagnet numerically by using real-space dynamical mean-field theory (RDMFT) [19], which can capture topological interfaces in interacting systems [20] and also invisible states as we need.

This Letter is arranged as follows: First, we briefly review the basic concepts about the zeros of the Green's function, and prove the existence of the invisible bands dual to the chiral edge modes in 2D Chern insulators. Then we introduce an interacting flat-band model, explain its ferromagnetic nature and present its mean-field (MF) domain-wall spectrum, which is later compared with the RDMFT results to identify the intrinsic interaction effect, i.e., the branching of the chiral domain-wall mode and the emergence of the invisible flat bands. Finally, we present an effective model to describe the domain-wall physics.

Zeros of the Green's function - In this Letter, the term Green's function refers to the zero-temperature single-particle Green's function of a fermionic many-body system with fixed number of particles N , whose formula can be found in the Supplemental Material (SM) [30]. For a fixed frequency ω , the Green's function \hat{G} is a d -by- d matrix whose matrix element G_{ij} is a Fourier component of the propagation amplitude between two single-particle states represented by i and j , where d is the dimension of the single-particle Hilbert space. The zeros of the Green's function \hat{G} are defined by the roots ω_m , $m = 1, 2, \dots, n_0$, of the equation $\det \hat{G}(\omega) = 0$. The vanishing of the determinant means that there is one or more null vectors of $\hat{G}(\omega_m)$, and we call the single-particle states corresponding to these null vectors *invisible states* with characteristic frequency ω_m , because they are decoupled from the rest of the single-particle states in terms of propagation amplitudes. In principle, the invisible states can be detected as long as $\hat{G}(\omega)$ can be measured, e.g., by angle-resolved photoemission spectroscopy (ARPES) for electronic systems, or by angle-resolved radio frequency spectroscopy for ultracold atoms [21].

Gurarie [18] proved that the determinant takes the following form:

$$\det \hat{G}(\omega) = \frac{\prod_{m=1}^{n_0} (\omega - \omega_m)}{\prod_{m=1}^{n_p} (\omega - \varepsilon_m)}, \quad (1)$$

where the poles ε_m are the eigenenergies of the many-particle Hamiltonian in the $(N+1)$ - and $(N-1)$ -particle space. He also showed that ω_m must be real numbers, and $n_p - n_0 = d$. In a closed non-interacting

system, we can easily calculate the Green's function and find $n_p = d$, hence $n_0 = 0$, which implies that zeros of the Green's function can only exist in open or interacting systems. Nevertheless, for any closed system, we can treat any of its subsystems as an open system, whose Green's function \hat{g} is a submatrix of \hat{G} . In this way, we can obtain new zeros of \hat{g} , which are not necessarily zeros of the full Green's function \hat{G} . Especially, if the subsystem is chosen as a topological interface, the emerging invisible bands associated with \hat{g} can carry information about the topology of the system, as we will discuss in the following.

Before we show this, we need to prove an important equation describing the configurations of the ω_m 's and ε_m 's in an S^1 parameter space of the system. Suppose the system is parameterized by a real number λ so that $\det \hat{G}(\omega, \lambda)$ is a *continuous* and *periodic* function of λ . Then we track the evolution of a pole, say $\varepsilon_1(\lambda)$, by increasing λ from λ_0 . Because of the periodicity of $\det \hat{G}(\omega, \lambda)$, $\varepsilon_1(\lambda)$ must either cease to exist at some $\lambda = \lambda_1$, or return to its initial value $\varepsilon_1(\lambda_0)$ after λ is swept over its whole period one or several times, otherwise, we will end up with infinitely many poles at any λ . In the former case, because the difference between the number of poles and zeros $n_p - n_0 = d$ is independent of λ , there must be one more zero at $\lambda_1 - 0^+$ than at $\lambda_1 + 0^+$. Let's denote this zero as $\omega_1(\lambda)$. Because $\det \hat{G}(\omega, \lambda)$ is a continuous function of λ , the pole and the zero must merge at λ_1 , i.e., $\omega_1(\lambda_1) = \varepsilon_1(\lambda_1)$. Then, we track $\omega_1(\lambda)$ by decreasing λ from λ_1 . Again, to avoid the existence of infinitely many zeros, $\omega_1(\lambda)$ ceases to exist at some point $\lambda = \lambda_2$, merging with either $\varepsilon_1(\lambda)$ or another pole $\varepsilon_2(\lambda)$. In the latter case, we can continue tracking $\varepsilon_2(\lambda)$ to another zero $\omega_2(\lambda)$ and so on, and finally we will return to $\varepsilon_1(\lambda_0)$ and complete a loop consisting of pole- and zero-branches. Note that every time a zero and a pole meet, the λ -direction of tracking reverses, so the path has a zig-zag shape. The key conclusion here is that any zero or pole is contained in such a loop (see Fig. 1(a) for some examples). Consider now a line with fixed $\omega = \Omega$. The line could possibly cut through one or several such loops and encounter poles and zeros at certain values Λ_i , $i = 1, 2, \dots$, i.e., $f(\lambda = \Lambda_i) = \Omega$ where f represents either a pole ε_m or a zero ω_m . We say it is a positive encounter at Λ_i if $f(\Lambda_i + 0^+) > \Omega > f(\Lambda_i - 0^+)$, and a negative encounter if $f(\Lambda_i + 0^+) < \Omega < f(\Lambda_i - 0^+)$. Due to the loop structure, the following equation holds [30]:

$$n_p^{(+)} - n_p^{(-)} = n_0^{(+)} - n_0^{(-)}, \quad (2)$$

where $n_p^{(\pm)}$ and $n_0^{(\pm)}$ denote the number of positively (negatively) encountered poles and zeros, respectively. This equation describes a topological property of $\det \hat{G}(\omega, \lambda)$ which holds for any system as long as λ lives in a S^1 space.

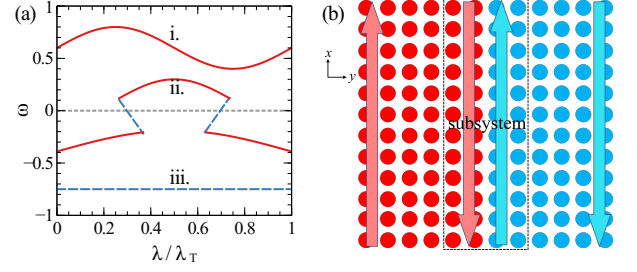


FIG. 1. (Color online) (a) Some possible configurations of poles and zeros as a function of λ , marked by red solid lines and blue dashed lines, respectively. The period of λ is λ_T . i. A loop consisting of a single pole. ii. A loop consisting of two poles and two zeros, forming a zig-zag path. iii. A loop consisting of a single zero. On the line $\omega = 0$, we find $n_p^+ = n_p^- = 0$ and $n_0^+ = n_0^- = 1$, so Eq. 2 holds. (b) Illustration of the ground state of H on a $2L \times 2L$ lattice with periodic boundary conditions filled with L^2 particles for each spin species. Sites half occupied by spin-up(down) particles are marked by red(blue) disks. There are two ferromagnetic domains separated by the domain walls. The arrows mark the domain-wall spin-current channels. The dashed rectangular marks the subsystem we choose to study the domain-wall physics.

Now, apply Eq. (2) to a 2D Chern insulator. Suppose the system is periodic along the x direction and has a topological interface in the y direction, e.g., an open boundary. In such a system, we can parameterize the Green's function $\hat{G}(\omega, k_x)$ by k_x , the momentum in the x direction. Instead of the whole system, we now focus on the subsystem defined as a stripe covering the topological interface. This subsystem has the Green's function $\hat{g}(\omega, k_x)$. Suppose the chemical potential sits in a band gap. If the chemical potential is crossed by in total C edge modes with the same chirality, which contribute C poles to $\det \hat{g}(\omega, k_x)$, Eq. (2) implies that there will also be C invisible bands of $\hat{g}(\omega, k_x)$ crossing the chemical potential with the same chirality, which establishes a one-to-one duality between zeros and poles at topological interfaces of 2D Chern insulators, with or without interaction. This is the first major result of this Letter.

Moreover, in the presence of interaction, the chiral edge modes can exhibit more sophisticated structures, e.g., they can be split into branches with new invisible bands connecting these branches of poles. Surprisingly, we find that these new invisible bands are flat in the model which we study in the following.

The model and the MF results - We study a 2D Hubbard model with repulsive interaction U :

$$H = \sum_{m,n,\sigma} h_{m,n} c_{m,\sigma}^\dagger c_{n,\sigma} + U \sum_m n_{m,\uparrow} n_{m,\downarrow} \quad (3)$$

in which $h_{m,n} \equiv t \exp\left(-\frac{|z_m - z_n|^2}{2} + i \text{Im } z_m^* z_n\right)$, $z_m \equiv \sqrt{S}(x_m + iy_m)$, $0 < S < \pi$, where (x_m, y_m) are the integer coordinates of the site m of a square lattice, and

we set $t = 1$. The non-interacting model, which has a zero-energy topological flat band, was first discovered by Kapit and Mueller [22]. The topological flat band in the non-interacting model can be regarded as the discrete lowest Landau level, and can be generalized to a family of topological flat bands [23–25]. For simplicity, we focus on the case $S = \pi/2$, in which the non-interacting model has only a flat lower band and a dispersive upper band. We only consider the filling ratio $1/4$. In this case, the ground state of the interacting model with $U > 0$ is fully ferromagnetic, i.e., all the spins are polarized and the flat band for the polarized spin will be fully occupied. The energy of such a state is zero because the flat band is at zero-energy and there is no interaction energy because of the polarization. A zero-energy state must be the ground state of H because H is positive semidefinite. The other ground states of H can be obtained by the spin $SU(2)$ symmetry.

Because the numbers of spin-up and spin-down particles are conserved quantities, we can fix them and let them be equal. Now, the ground state is no longer homogeneous. The lattice is split into two ferromagnetic domains to lower the energy, and the ground state seeks the shortest domain wall. Consider a $2L \times 2L$ lattice with periodic boundary conditions in both directions. Then, there are L^2 particles for each spin species, and the domain walls will be formed as shown in Fig. 1(b).

Consider the MF theory for the spin-up single-particle excitations of the ground state. The MF Hamiltonian is obtained by treating the interaction term $U \sum_m n_{m,\uparrow} n_{m,\downarrow}$ as a background potential $U \sum_m n_{m,\uparrow} \langle n_{m,\downarrow} \rangle$, which removes the entanglement between the two spin species. The MF theory gives the correct ground-state energy only when U is small compared to the gap between the two bands in the non-interacting model. Deep in the spin-up domain, the background potential vanishes because no spin-down particle is present, and deep in the spin-down domain, the potential becomes $U/2$ because each site holds on average half of a spin-down particle. As a result, apart from the contribution from the domain walls, the MF spectrum is obtained by duplicating the spectrum of the non-interacting model and shifting the duplicate by $\Delta = U/2$, the gap between the two flat bands in the different domains. The topological bands will contribute chiral modes to the domain wall, and the domain wall becomes a spin current channel (see Fig. 1(b)), which is called quantum valley Hall effect in some works [26–29]. To visualize the domain-wall modes and their dual invisible bands, we exactly diagonalize the MF Hamiltonian on a 64×64 lattice with periodic boundary conditions, choose the subsystem as a 4-site-width stripe over the domain wall, and calculate the determinant $\det \hat{g}^{(\uparrow)}(\omega + 0^+ i, k_x)$ (Fig. 2(a)) and the domain-wall spin-up spectral function $\sum_y \text{Im } g_{yy}^{(\uparrow)}(\omega + 0^+ i, k_x)$ (Fig. 2(e)), where the summation only takes values of y within the subsystem. We see that cross-shaped invisible

bands appear, which makes Eq. (2) hold.

RDMFT analysis on interacting system - RDMFT is an extension of the single-site DMFT to deal with inhomogeneity in a correlated lattice system. It solves the lattice many-body problem by reducing the full problem to a set of single impurity problems, one for each lattice site, with the impurity Green's function and self-energy being the same as those of the respective site. These impurity problems are coupled via the lattice Dyson equation,

$$\left[\hat{G}^{(\sigma)}(\omega) \right]_{m,n}^{-1} = \omega + \mu - h_{m,n} - \delta_{m,n} \Sigma_n^{(\sigma)}(\omega), \quad (4)$$

where μ is the chemical potential, $h_{m,n}$ is defined below Eq. (3), and $\Sigma_n^{(\sigma)}(\omega)$ is the site-dependent local self-energy, while the non-local parts of the self-energy are neglected in the approximation. We apply RDMFT to a lattice with 64×64 sites and periodic boundary conditions. Because RDMFT is formulated in the grand canonical ensemble, the number of spin-up or spin-down particles cannot be fixed. In order to form two ferromagnetic domains and keep the numbers of spin-up and spin-down particles equal, we initiate the RDMFT iterations with a slightly biased chemical potential to attract the spin-up(down) particles to the left(right) half of the lattice, and the bias is removed after the first iteration. This initial condition leads to a well converged solution from which we read that the magnetization $|\langle n_{n,\uparrow} - n_{n,\downarrow} \rangle|$ is $\frac{1}{2}$ for site n in each domain. We also find that the spectrum does not change qualitatively when the interaction strength U varies, therefore in the following we only present the results for $U = 2$. The inverse temperature is set as $\beta = 200$, which makes the results effectively characterize zero-temperature physics.

In Fig. 2(h), the x -momentum-integrated spin-up spectral density $\sum_{k_x} \text{Im } G_{yy}^{(\uparrow)}(\omega + 0^+ i, k_x)$ calculated by RDMFT clearly distinguishes the two domains. The flat bands survive the interaction, however, the gap between them $\Delta = 0.67$ is much smaller than the MF value $U/2 = 1$. The chemical potential is chosen as half the gap, $\mu = \Delta/2 = 0.33$. As a result, in the spin-up domain, we have poles located at $\omega = -\mu$ corresponding to creating holes in the filled spin-up flat band. And, in the spin-down domain, we have poles located at $\omega = \mu$ corresponding to creating spin-up particles in the filled spin-down flat band. Further numerical results show that Δ is a monotonous function of U , $\Delta \rightarrow U/2$ when $U \rightarrow 0$, and $\Delta < \Delta_{\max} \approx 1.4$ when $U \rightarrow \infty$ [30], which means that Δ is always smaller than the band gap of the non-interacting model, preventing a qualitative change of the spectrum. Δ_{\max} is verified by exact diagonalization (ED) of the Hamiltonian on a 4×4 lattice, and we find that the ED results agree surprisingly well with RDMFT in the sense that for any U , the relative difference in Δ is about 1% [30].

The subsystem containing the domain wall is again chosen as a 4-site-width stripe. We show the

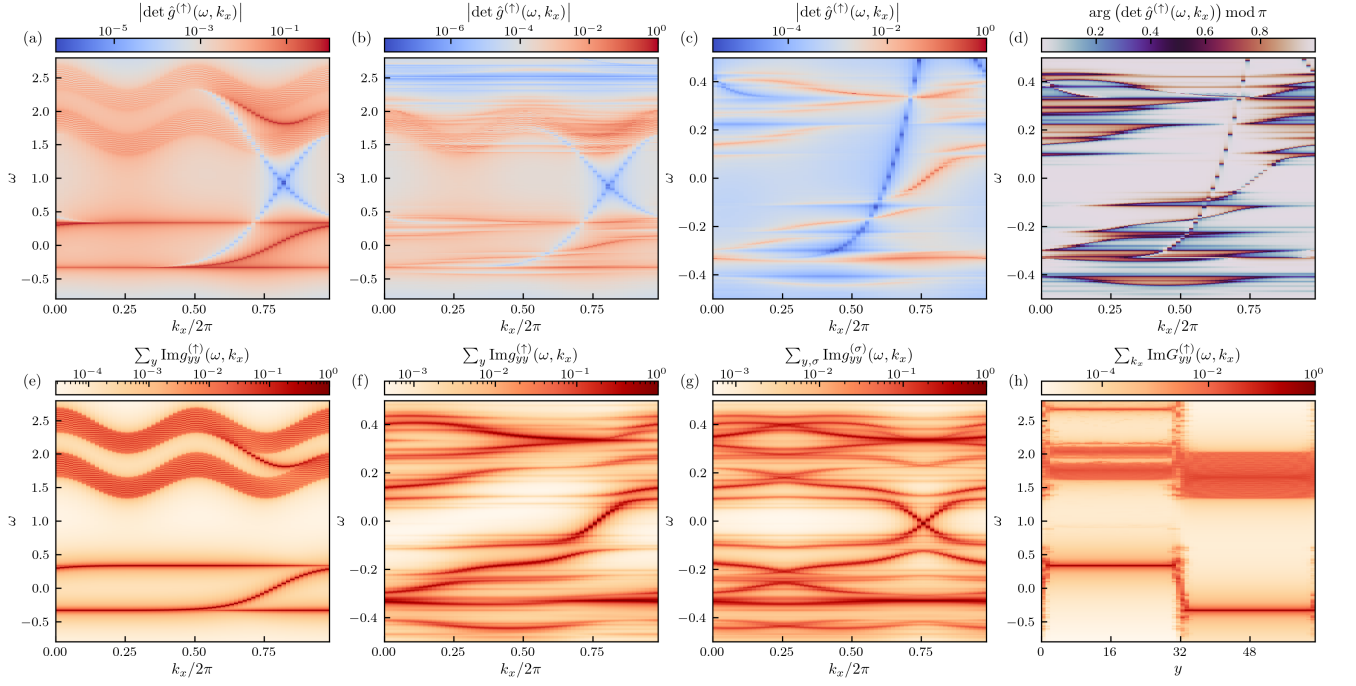


FIG. 2. (Color online) The Green's functions $\hat{g}(\omega, k_x)$ (subsystem) and $\hat{G}(\omega, k_x)$ (full system) calculated by (a)(e) MF theory and (b-d)(f-h) RDMFT. (a-d) plot $\det \hat{g}$ to show the invisible bands (the darkest blue lines in (a-c)) and (e-h) plot the y -summed spectral densities to show the poles (the darkest red lines), including the chiral domain-wall modes. The system size is 64-by-64, and U is set as 1.33 for MF and 2 for RDMFT such that they produce the same gap $\Delta = 0.67$. There are two ω -ranges. The larger range includes all the bulk bands in MF results, and the smaller range resolves the details of domain-wall states.

RDMFT determinant $\det \hat{g}(\omega + 0^+i, k_x)$ in Fig. 2(b-d) and the RDMFT domain-wall spin-up spectral function $\sum_y \text{Im} g_{yy}^{(\uparrow)}(\omega + 0^+i, k_x)$ in Fig. 2(f). Comparing Fig. 2(e) with Fig. 2(f), we find the chiral domain-wall mode is split into multiple branches by the interaction, and these branches, as shown in Fig. 2(c-d), are connected by branches of invisible bands. The zig-zag path formed by the branches can be more clearly distinguished by the argument of $\det \hat{g}(\omega + 0^+i, k_x)$ in Fig. 2(d). Strikingly, these branches of invisible bands are flat. Note that any linear superposition of invisible states in the invisible flat band is an invisible state with the same characteristic frequency. Moreover, these invisible bands, as the manifestation of quantum correlation, exist even in the full Green's function. The existence of invisible flat bands is the other major result of this Letter.

In Fig. 2(f), if we draw a line with a fixed $\omega \in (-\frac{\Delta}{2}, \frac{\Delta}{2})$, the line will encounter one and only one pole, which means the bulk-edge correspondence isn't broken by the interaction. In Fig. 2(b), we see that the two cross-shaped major invisible bands almost remain the same as those in the MF calculation, being more stable than the chiral modes with respect to interaction. In this sense, invisible bands may serve as a better indicator for detecting interacting 2D Chern insulators.

Last but not least, by summing up the spin-up and the spin-down spectral functions, we obtain Fig. 2(g) and

find that the spin-up and spin-down chiral modes connect smoothly and form bands extending over the whole Brillouin zone. This fact inspires us to depict the domain-wall states by a 1D single-particle model where the interaction is effectively replaced by spin mixing, i.e., a spin-up particle can turn into a spin-down one by hopping and vice versa. The effective model is supposed to reproduce the branching in the domain-wall spectrum. The simplest effective model contains two bands $\varepsilon_{\pm}(k)$ associated with eigenstates $|u_k^+\rangle = \alpha(k)|\uparrow\rangle + \beta(k)|\downarrow\rangle$ and $|u_k^-\rangle = \beta^*(k)|\uparrow\rangle - \alpha^*(k)|\downarrow\rangle$, and it is straightforward to generalize the two-band effective model to a multi-band one to account for more branches. The single-particle effective Hamiltonian is $h(k) = \sum_{\delta=\pm} \varepsilon_{\delta}(k) |u_k^{\delta}\rangle \langle u_k^{\delta}|$ and the corresponding spin-up Green's function is

$$g_{\text{eff}}^{(\uparrow)}(\omega, k) = \frac{\gamma(k)}{\omega - \varepsilon_+(k)} + \frac{1 - \gamma(k)}{\omega - \varepsilon_-(k)}, \quad (5)$$

where $\gamma(k) = |\alpha(k)|^2$. The poles $\varepsilon_{\pm}(k)$ are split into branches when $\gamma(k) = 0$ or 1 in part of the Brillouin zone, and the invisible band connecting the poles is given by $\omega(k) = \gamma(k)\varepsilon_-(k) + (1 - \gamma(k))\varepsilon_+(k)$, existing in the region where $0 < \gamma(k) < 1$ [30]. Apparently, it puts a strong constraint on the Hamiltonian if we require this invisible band to be flat.

Conclusion - Using RDMFT, we numerically study the ferromagnetic ground state and its domain walls of a

repulsive Hubbard model, in which the ferromagnetism comes from the topological flat band of the underlying non-interacting model. Our results show that the flat bands survive the interaction and they contribute chiral modes to the domain walls because of their non-trivial topology. The chiral modes are associated with the poles of the Green's function of the domain wall \hat{g} . Moreover, \hat{g} also possesses zeros associated with invisible bands. We analyse the configurations of zeros and poles of Green's functions, and rigorously prove that there is a one-to-one duality between the chiral modes and invisible bands at topological interfaces of 2D Chern insulators. Therefore, the invisible bands can also serve as indicators of non-trivial topology. Our numerical results agree with this analysis, clearly showing the invisible bands dual to the domain-wall modes. Moreover, the RDMFT results show that the domain-wall modes are split into branches, an effect which is not present in the MF results, suggesting that the branching is intrinsically caused by quantum correlations. The branching can be captured by a 1D effective model with spin-mixing. Both the numerical and analytical study show that the branches of domain-wall modes are connected by invisible bands, and RDMFT shows that these invisible bands are flat. The flatness of these invisible bands puts strong constraints on the Hamiltonian, and could be closely related to the flat bands in the non-interacting model.

We thank Arijit Dutta for discussion. This work was supported by the Deutsche Forschungsgemeinschaft (DFG, German Research Foundation) under Project No. 277974659 via Research Unit FOR 2414. This work was also supported by the DFG via the high performance computing center *Center for Scientific Computing* (CSC).

-
- [1] H. Tasaki, *Prog. Theor. Phys.* **99**, 489 (1998).
 - [2] Z. Gulácsi, A. Kampf, and D. Vollhardt, *Phys. Rev. Lett.* **99**, 026404 (2007).
 - [3] E. H. Lieb, *Phys. Rev. Lett.* **62**, 1201 (1989).
 - [4] A. Mielke, *J. Phys. A Math. Theor.* **25**, 4335 (1992).
 - [5] H. Tasaki, *Phys. Rev. Lett.* **69**, 1608 (1992).

- [6] R. Liu, W. Nie, and W. Zhang, *Sci. Bull.* **64**, 1490 (2019).
- [7] H. Katsura, I. Maruyama, A. Tanaka, and H. Tasaki, *EPL* **91**, 57007 (2010).
- [8] T. Neupert, L. Santos, S. Ryu, C. Chamon, and C. Mudry, *Phys. Rev. Lett.* **108**, 046806 (2012).
- [9] A. Zhao and S.-Q. Shen, *Phys. Rev. B* **85**, 085209 (2012).
- [10] E. J. Bergholtz and Z. Liu, *Int. J. Mod. Phys. B* **27**, 1330017 (2013).
- [11] N. Regnault and B. A. Bernevig, *Phys. Rev. X* **1**, 021014 (2011).
- [12] Z. Liu, E. J. Bergholtz, and E. Kapit, *Phys. Rev. B* **88**, 205101 (2013).
- [13] D. N. Sheng, Z.-C. Gu, K. Sun, and L. Sheng, *Nat. Commun.* **2**, 389 (2011).
- [14] T. Neupert, L. Santos, C. Chamon, and C. Mudry, *Phys. Rev. Lett.* **106**, 236804 (2011).
- [15] L. S. G. Leite and R. L. Doretto, *Phys. Rev. B* **104**, 155129 (2021).
- [16] X.-F. Su, Z.-L. Gu, Z.-Y. Dong, S.-L. Yu, and J.-X. Li, *Phys. Rev. B* **99**, 014407 (2019).
- [17] S. S. Pershoguba and V. M. Yakovenko, *Phys. Rev. B* **105**, 064423 (2022).
- [18] V. Gurarie, *Phys. Rev. B* **83**, 085426 (2011).
- [19] M. Snoek, I. Titvinidze, C. Tóke, K. Byczuk, and W. Hofstetter, *New J. Phys.* **10**, 093008 (2008).
- [20] B. Irsigler, J.-H. Zheng, and W. Hofstetter, *Phys. Rev. Lett.* **122**, 010406 (2019).
- [21] W. Hofstetter and T. Qin, *J. Phys. B. Atom. Molec. Opt. Phys.* **51**, 082001 (2018).
- [22] E. Kapit and E. Mueller, *Phys. Rev. Lett.* **105**, 215303 (2010).
- [23] H. Atakışi and M. O. Oktel, *Phys. Rev. A* **88**, 033612 (2013).
- [24] J. Dong and E. J. Mueller, *Phys. Rev. A* **101**, 013629 (2020).
- [25] Y. Xu and H. Pu, *Phys. Rev. A* **102**, 053305 (2020).
- [26] M. Tahir, A. Manchon, K. Sabeeh, and U. Schwingenschlögl, *Appl. Phys. Lett.* **102**, 162412 (2013), <https://doi.org/10.1063/1.4803084>.
- [27] M. Ezawa, *Phys. Rev. B* **88**, 161406 (2013).
- [28] T. Ma and G. Shvets, *New J. Phys.* **18**, 025012 (2016).
- [29] J. Liu, Z. Ma, J. Gao, and X. Dai, *Phys. Rev. X* **9**, 031021 (2019).
- [30] Supplemental Material, which includes an introduction to the Green's function and its determinant, a proof of Eq. (2), a fit to the Δ - U curve obtained by RDMFT, some ED results, and an example of the 1D effective model.

Supplemental material: Invisible flat bands on a topological chiral edge

Youjiang Xu, Irakli Titvinidze, Walter Hofstetter
Institut für Theoretische Physik, Goethe-Universität, 60438 Frankfurt am Main, Germany

I. GREEN'S FUNCTION AND ITS DETERMINANT

In a zero-temperature fermionic many-body system which conserves the number of particles, the time-ordered single-particle Green's function is given by the following formula:

$$G_{ij}(t) = -i \langle N, 0 | T c_i(t) c_j^\dagger | N, 0 \rangle, \quad (S1)$$

where $c_i(t)$ is the fermionic annihilator for state i at time t , T is the time ordering operator, and $|N, 0\rangle$ denotes the ground state with N particles. N can be adjusted by setting the chemical potential included in the Hamiltonian. And, by adding a constant to the Hamiltonian, we can shift the ground state energy to zero, and all the other eigenenergies of the Hamiltonian will be non-negative. Under these conditions, the Green's function in the frequency domain used in the Letter is given by

$$G_{ij}(\omega) = \int_{-\infty}^{\infty} e^{i\omega t} G_{ij}(t) dt \\ = \sum_n \frac{\langle N, 0 | c_i | N+1, n \rangle \langle N+1, n | c_j^\dagger | N, 0 \rangle}{\omega - E_{N+1, n} + 0^+ i} \quad (S2)$$

$$+ \sum_n \frac{\langle N, 0 | c_j^\dagger | N-1, n \rangle \langle N-1, n | c_i | N, 0 \rangle}{\omega + E_{N-1, n} - 0^+ i}, \quad (S3)$$

where $|N \pm 1, n\rangle$ denotes the eigenstates of the Hamiltonian with one more or less particles than the ground state. This formula can be written in a compact form:

$$G_{ij}(\omega) = \sum_m \frac{U_{m,i} U_{m,j}^*}{\omega - \varepsilon_m}, \quad (S4)$$

where ε_m can either represent $E_{N+1, n}$ or $-E_{N-1, n}$, and $U_{m,i}$ can either represent $\langle N, 0 | c_i | N+1, n \rangle$ or $\langle N-1, n | c_i | N, 0 \rangle$. The completeness of the states $|N \pm 1, n\rangle$ in their respective particle number spaces implies that $U_{m,i}$ satisfies the following equation:

$$\sum_m U_{m,i} U_{m,j}^* = \delta_{ij}. \quad (S5)$$

Now consider the form of $\det \hat{G}(\omega)$. We denote the dimension of the single-particle Hilbert space as d , which also equals the number of orthonormal single-particle states i corresponding to the operators c_i . In a non-interacting closed system, there exists a set of c_i such that each i corresponds to one eigenstate of the single-particle Hamiltonian and $U_{m,i} = \delta_{m,i}$. In this case, $\det \hat{G}(\omega) = \prod_{m=1}^{n_p} (\omega - \varepsilon_m)^{-1}$ where $n_p = d$ is the number of poles in $\det \hat{G}(\omega)$. For general c_i 's, $U_{m,i}$ will be a unitary matrix, and $\det \hat{G}(\omega)$ is invariant under transformation of basis. Therefore, $\det \hat{G}(\omega)$ has no zeros for a non-interacting closed system.

For an interacting or open system, zeros can show up. The asymptotic behavior of the determinant is given by $\det \hat{G}(\omega) \rightarrow \omega^{-d}$ when $\omega \rightarrow \infty$, so $\det \hat{G}(\omega)$ can no longer be $\prod_{m=1}^{n_p} (\omega - \varepsilon_m)^{-1}$, which drops faster than ω^{-d} in an interacting or open system because $n_p > d$. Intuitively, we expect $\prod_{m=1}^{n_p} (\omega - \varepsilon_m)^{-1}$ should be multiplied by a degree- $(n_p - d)$ polynomial $\prod_{m=1}^{n_p-d} (\omega - \omega_m)$ to reproduce the correct asymptotic behavior, where ω_m 's are some complex numbers. Indeed, it was rigorously proved that [1]

$$\det \hat{G}(\omega) = \frac{\prod_{m=1}^{n_p-d} (\omega - \omega_m)}{\prod_{m=1}^{n_p} (\omega - \varepsilon_m)}, \quad (S6)$$

where ω_m are real numbers.

TABLE S1. Δ calculated by ED and RDMFT

U	1	10	100
Δ (ED)	0.410	1.194	1.382
Δ (RDMFT)	0.408	1.180	1.366

II. PROOF OF EQ. (2) IN THE MAIN TEXT

Consider a loop composed of branches of zeros $\omega_m(\lambda)$ and poles $\varepsilon_m(\lambda)$ in the S^1 -space of λ , where $m = 1, 2, \dots, n_b$. It is straightforward to generalize the proof to the case in which the loop consists of a single zero or pole. Suppose $\varepsilon_m(\lambda)$ merges with $\omega_m(\lambda)$ at λ_{2m-1} , $\omega_m(\lambda)$ merges with $\varepsilon_{m+1}(\lambda)$ at λ_{2m} , where $\varepsilon_{n_b+1}(\lambda)$ is defined as $\varepsilon_1(\lambda)$. Without loss of generality, we assume $\lambda_1 > \lambda_0 \equiv \lambda_{2n_b}$, and we parameterize the loop by $\tau \in [0, 1)$ in the following way:

$$\tilde{\lambda}(\tau) \equiv (\lambda_m - \lambda_{m-1})(2n_b\tau - m) + \lambda_m, \quad \tau \in \left[\frac{m-1}{2n_b}, \frac{m}{2n_b}\right), \quad m = 1, 2, \dots, 2n_b, \quad (\text{S7})$$

and

$$\tilde{\omega}(\tau) \equiv \begin{cases} \varepsilon_m(\tilde{\lambda}(\tau)), & \tau \in \left[\frac{2m-2}{2n_b}, \frac{2m-1}{2n_b}\right) \\ \omega_m(\tilde{\lambda}(\tau)), & \tau \in \left[\frac{2m-1}{2n_b}, \frac{2m}{2n_b}\right) \end{cases}, \quad m = 1, 2, \dots, n_b. \quad (\text{S8})$$

Now, consider a line $\omega = \Omega$. We say that $\tilde{\omega}(\tau)$ positively encounters the line at T if $\tilde{\omega}(T+0^+) > \tilde{\omega}(T) = \Omega > \tilde{\omega}(T-0^+)$, and that $\tilde{\omega}(\tau)$ negatively encounters the line at T if $\tilde{\omega}(T+0^+) < \tilde{\omega}(T) = \Omega < \tilde{\omega}(T-0^+)$. Similarly, we can define the positive or negative encounter of a zero or pole with the line $\omega = \Omega$. Let $f(\lambda)$ represent either a pole $\varepsilon_m(\lambda)$ or a zero $\omega_m(\lambda)$. We say that $f(\lambda)$ positively encounters the line at Λ if $f(\Lambda+0^+) > f(\Lambda) = \Omega > f(\Lambda-0^+)$, and that $f(\lambda)$ negatively encounters the line at Λ if $f(\Lambda+0^+) < f(\Lambda) = \Omega < f(\Lambda-0^+)$. As long as the line $\omega = \Omega$ doesn't meet any merging point, i.e., $\Omega \neq \omega_m(\lambda_{2m-1})$ and $\Omega \neq \omega_m(\lambda_{2m})$ for any m , then a positive encounter of $\tilde{\omega}(\tau)$ is either a positive encounter of a pole, or a negative encounter of a zero, because $\tilde{\lambda}'(\tau)$ is always positive for a pole and negative for a zero due to the assumption $\lambda_1 > \lambda_0$. Therefore, the number of positive encounters of $\tilde{\omega}(\tau)$, $n^{(+)}$, equals $n_p^{(+)} + n_0^{(-)}$, where $n_p^{(\pm)}$ and $n_0^{(\pm)}$ denote the number of positively(negatively) encountered poles and zeros, respectively. Similarly, we have $n^{(-)} = n_p^{(-)} + n_0^{(+)}$. Since $\tilde{\omega}(\tau)$ is a loop, we have $n^{(+)} = n^{(-)}$, or:

$$n_p^{(+)} + n_0^{(-)} = n_p^{(-)} + n_0^{(+)}, \quad (\text{S9})$$

which is identical with Eq. (2) in the main text.

III. FIT THE GAP CALCULATED BY RDMFT

We find a simple function to fit the gap Δ calculated by RDMFT as a function of U :

$$\Delta = \frac{A_0}{2} \tanh \frac{U}{A_0 + A_1 U}, \quad (\text{S10})$$

in which the fitting parameters are given by $A_0 = 2.976$ and $A_1 = 0.619$. Note that the fitting function is approximated by $\Delta = U/2$ at small U , and is bounded by $\frac{A_0}{2} \tanh \frac{1}{A_1} = 1.375$ for $U \rightarrow \infty$. We compare the RDMFT results with the fitting function in Fig. S1

IV. COMPARISON OF THE GAP CALCULATED BY ED AND RDMFT

In Table. S1, we list Δ , the gap between the two flat bands in the different domains, calculated by ED and RDMFT. The results obtained by the two methods show very good agreement.

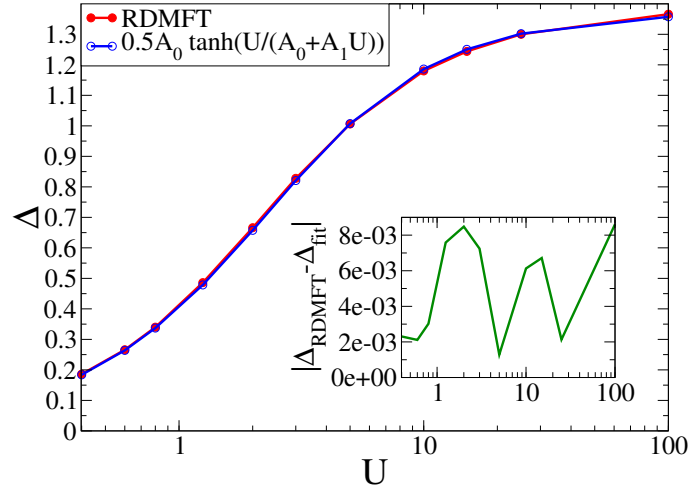


FIG. S1. (Color online) The gap Δ as a function of U . The red closed circles are the RDMFT results while the blue open circles are given by the fitting function. The difference between the two is shown in the inset panel.

V. 1D EFFECTIVE MODEL FOR THE DOMAIN WALL: AN EXAMPLE

As discussed in the main text, the branching of the chiral domain-wall mode can be captured by a non-interacting effective model in which the interaction is effectively replaced by spin-mixing. Here we show a two-band model as a specific example. Suppose the two bands are given by

$$\varepsilon_+(k) = 1 + \frac{1}{2} \sin k, \quad (\text{S11})$$

$$\varepsilon_-(k) = -1 + \frac{1}{2} \cos k. \quad (\text{S12})$$

The single-particle effective Hamiltonian is $h(k) = \sum_{\delta=\pm} \varepsilon_{\delta}(k) |u_k^{\delta}\rangle \langle u_k^{\delta}|$ where the eigenstates are given by

$$|u_k^+\rangle = \alpha(k) |\uparrow\rangle + \beta(k) |\downarrow\rangle \quad (\text{S13})$$

$$|u_k^-\rangle = \beta^*(k) |\uparrow\rangle - \alpha^*(k) |\downarrow\rangle \quad (\text{S14})$$

in which

$$\alpha(k) = \theta(\cos k) + \theta(-\cos k) \theta(-\cos 2k) \cos 2k, \quad (\text{S15})$$

$$\beta(k) = \theta(-\cos k) (\theta(\cos 2k) + \theta(-\cos 2k) \sin 2k). \quad (\text{S16})$$

where θ is the step function: $\theta(x) = 1$ if $x \geq 0$, and $\theta(x) = 0$ if $x < 0$. We show the branches of poles and zeros of this model in Fig. S2.

[1] V. Gurarie, *Phys. Rev. B* **83**, 085426 (2011).

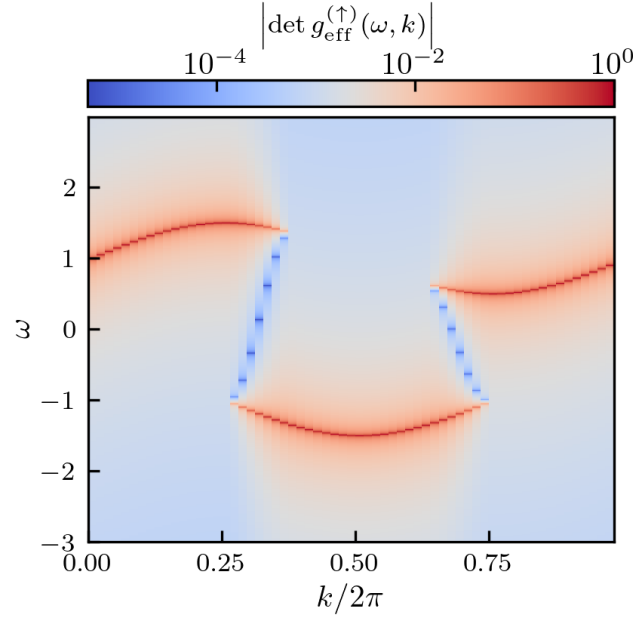


FIG. S2. (Color online) The branches of zeros and poles of the Green's function of the 1D effective model defined in Eq. (S11-S16).